

The impact of vegetation on REE fractionation in stream waters of a small forested catchment (the Strengbach case)

P. Stille^{a,*}, M. Steinmann^b, M.-C. Pierret^a, F. Gauthier-Lafaye^a, F. Chabaux^a,
D. Viville^a, L. Pourcelot^c, V. Matera^d, G. Aouad^a, D. Aubert^{a,e}

^a CGS, CNRS, UMR 7517, EOSt, F-67084 Strasbourg, France

^b EA 2642 Géosciences, Université de Franche-Comté, F-25030 Besançon, France

^c Institut de Radioprotection et de Sécurité Nucléaire IRSN, Cadarache, F-13108 St. Paul Lez Durance, France

^d Inst. Géol., Université de Neuchâtel, CH-2007 Neuchâtel, Switzerland

^e CEFREM, UMR 5110, Université de Perpignan, F-66860 Perpignan, France

Received 15 September 2005; accepted in revised form 26 April 2006

Abstract

Previous studies on waters of a streamlet in the Vosges Mountains (Eastern France) have shown that strontium and rare earth elements (REE) mainly originate from preferential dissolution of apatite during weathering. However, stream water REE patterns normalized to apatite are still depleted in the light REE (LREE, La–Sm) pointing to the presence of an additional LREE depleting process. Vegetation samples are strongly enriched in LREE compared to stream water and their Sr and Nd isotopic compositions are comparable with those of apatite and stream water. Thus, the preferential LREE uptake by vegetation might lead to an additional LREE depletion of surface runoff in the forested catchment. Mass balance calculations indicate, that the yearly LREE uptake by vegetation is comparable with the LREE export by the streamlet and, therefore, might be an important factor controlling LREE depletion in river water. This is underlined by the observation that rivers from arctic and boreal regions with sparse vegetation appear to be less depleted in LREE than rivers from tropical environments or boreal environments with a dense vegetation cover.

© 2006 Elsevier Inc. All rights reserved.

1. Introduction

Natural waters are the main pathway for the transport of elements and particles from the surface and subsurface of the continents to the oceans. Their chemical and isotopic composition is the result of interaction with the environment and especially controlled by erosional processes. Therefore, major river systems have been studied to estimate the fluxes of continent-derived material to the oceans and to shed light upon erosion processes on a global scale (Martin and Meybeck, 1979; Stallard and Edmond, 1983; Meybeck, 1987; Négrel et al., 1993; Blum et al., 1994; Gaillardet et al., 1995, 1997; Dupré et al., 1996). Alteration leads to the disaggregation of rocks and minerals, the for-

mation of soils and also allows the removal of chemical elements as well as of larger and smaller particles from altered rocks and soils by surface runoff. Previous studies have shown that REE are powerful geochemical tracers that provide information about the origin of the suspended and the dissolved river load and about elemental fractionation between particulate and solution phases (Goldstein et al., 1984; Stordal and Wasserburg, 1986; Goldstein and Jacobsen, 1987, 1988a,b; Elderfield et al., 1990; Sholkovitz, 1992; Allègre et al., 1996; Tricca et al., 1999; Stille et al., 2003). The fractionation of the REE in river water between dissolved and particulate load as well as immobilization of the REE in the river sediment can be extensive and is strongly controlled by weathering reactions, surface adsorption and solution chemistry (Sholkovitz, 1995; Byrne and Sholkovitz, 1996; Byrne and Liu, 1998). With the exception of Ce (IV) the lanthanides have trivalent

* Corresponding author. Fax: +33 03 90 240 402.
E-mail address: pstille@illite.u-strasbg.fr (P. Stille).

oxidation state in most natural waters. The elements of the lanthanide series are characterized by a gradual decrease in the ionic radii with increasing atomic number (“lanthanide contraction” from La^{3+} to Lu^{3+} ; e.g., Brookins, 1989) leading to a slightly different behavior for heavy REE (HREE, Dy–Lu) and light REE (LREE, La–Sm) during chemical processes such as coprecipitation, adsorption or complexation. The configuration of the valence electrons does not change throughout the series because the additional electrons are systematically filled into the f-electron shell. From the literature it is known that competition between free and complexed REE ions, surface adsorption as well as REE scavenging by colloidal particles may strongly fractionate the relative lanthanide concentrations (Byrne and Kim, 1990; Byrne and Li, 1995; Byrne and Sholkovitz, 1996). As a consequence, REE concentrations in natural waters and fractionation of their distribution patterns strongly depend on pH, availability of potential complex ligands, and the presence of particles and colloids (Byrne and Sholkovitz, 1996).

Besides weathering, solution and surface chemistry, other factors such as vegetation have rarely been considered to be of importance for the REE distributions in river water although plants are actually known to accumulate REE under natural conditions (Sun et al., 1999; Yang et al., 1999; Zhimang et al., 2000; Ozaki and Enomoto, 2001; Akagi et al., 2002; Krachler et al., 2003). Therefore, vegetation might, especially in tropical and temperate zones, be an important REE sink potentially capable of fractionating the REEs in surface runoff. The aim of the present study is to determine in how far vegetation may fractionate the relative lanthanide concentrations in natural surface waters. To do this, the Strengbach streamlet and its uppermost catchment in the Vosges mountains (France) has been chosen, because the isotopic and REE characteristics of this site have already previously been extensively studied (Amiotte-Suchet et al., 1999; Riotte and Chabaux, 1999; Tricca et al., 1999; Aubert et al., 2001, 2002a,b, 2004).

2. Site setting

The Strengbach forested catchment covering an area of 80 ha is located in the eastern part of the Vosges mountains (Northeastern France) at altitudes ranging from 883 m at the outlet to 1146 m at the top (Fig. 1). This uppermost catchment site of the Strengbach has been thoroughly investigated since 1986 and has become a completely equipped environmental observatory with permanent sampling and measuring stations (<http://ohge.u-strasbg.fr>). A review of earlier geochemical, mineralogical and biological studies realized on the site is given by Probst et al. (1990) and Aubert et al. (2002a). The bedrock of the catchment is a homogeneous Hercynian leucogranite. Temperate oceanic mountainous climate with west wind dominates. The monthly averages of daily mean temperatures range from $-2\text{ }^{\circ}\text{C}$ to $14\text{ }^{\circ}\text{C}$ (Probst et al., 1990). Rainfall occurs over the whole year with an annual average of 1400 mm

(Probst et al., 1995). The forest is dominated by conifers (80%) and beech (20%). The average annual stream discharge is about $680,000\text{ m}^3/\text{year}$. Weathering products and secondary mineral phases in soils and saprolite have previously been characterized (El Gh’Mari, 1995; Fichter et al., 1998). Hydrological processes have been studied extensively (Viville et al., 1993; Lu et al., 1995; Idir et al., 1999; Ladouche et al., 2001; Aubert et al., 2002a). After leaving the uppermost catchment and during its travel of about 15 km down to the Rhine valley, the Strengbach stream crosses different lithologies and mixes up with smaller influent streams from adjoining catchments. As a consequence, pH and major element composition of stream water evolve from upstream to downstream (Riotte and Chabaux, 1999; Tricca et al., 1999).

3. Analytical methods

The water samples were filtered on site through $0.45\text{ }\mu\text{m}$ pore size Millipore cellulose acetate filters. The solution which passed this filter is called the dissolved load and includes dissolved ions and $<0.45\text{ }\mu\text{m}$ colloids. The filtered samples were acidified with bidistilled HCl to pH 1–2 and stored in acid-cleaned HDPE bottles. The solid sample fraction ($>0.45\text{ }\mu\text{m}$; suspended load) as well as bottom sediments and soils were considered to consist of two major phases: an unleachable residue and a leachable pool (Sholkovitz et al., 1994).

Leaching experiments with 1 N HCl at room temperature for 15 min have been performed on soil samples, stream water particles ($>0.45\text{ }\mu\text{m}$) and bottom sediments in order to recover the leachable pool which is considered to represent adsorbed REE and REE fixed in HCl-soluble mineral phases such as Fe–Mn oxy-hydroxides (Steinmann and Stille, 1997). Some of these HCl leachable cations can under natural conditions potentially go into solution and enter surface and subsurface runoff. Of course, the unleachable detritus and the leachable pool are operationally defined because there is always a continuum between leachable and residual phases (Stille and Clauer, 1994; Steinmann and Stille, 1997).

The REE concentrations of the filtered water samples ($<0.45\text{ }\mu\text{m}$) are below the detection limit of traditional quadrupole ICP MS ($0.01\mu\text{g/L}$) and therefore a specific enrichment method was required. A liquid–liquid extraction technique using HDEHP as organic solvent has been applied to enrich the REE by a factor of at least 100 (Shabani and Masuda, 1991; Tricca, 1997; Tricca et al., 1999). Some 0.5–2 L of samples was necessary to achieve concentrations above detection limit. The same extraction technique has been used to obtain sufficient Nd (at least 20 ng) for isotope determinations. The cations have been measured by AAS with a Perkin-Elmer 430 Spectrometer and the anions with a Dionex Ionic Chromatograph. The error is less than 1% for both analyses. A Shimadzu TOC 5000 apparatus has been used to determine DOC (dissolved organic carbon) concentrations.

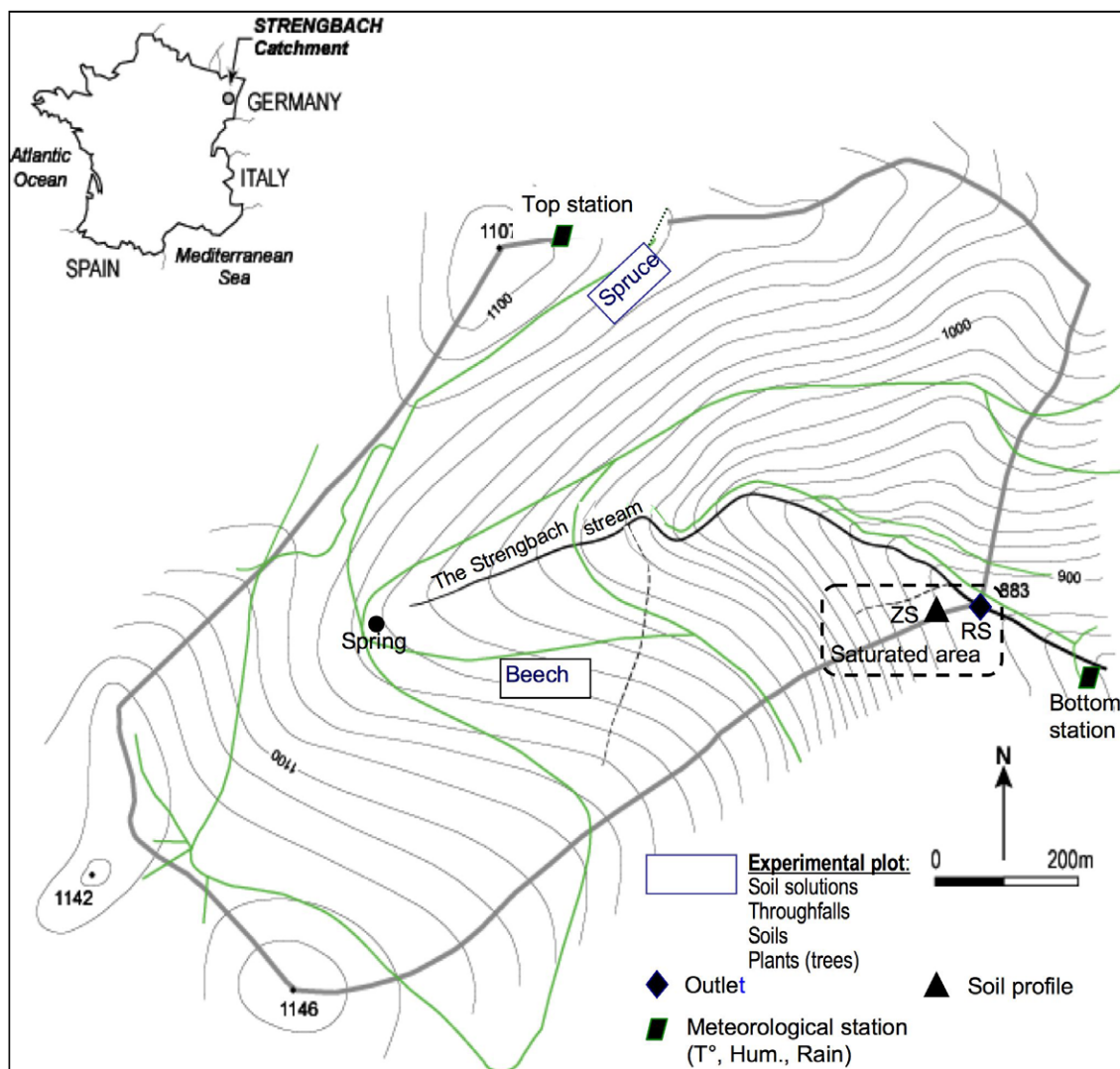


Fig. 1. Uppermost Strengbach catchment with sampling sites. ZS: soil profile in the water saturated zone close to the catchment outlet.

Throughfall has been collected under conifers using 2 m-long open gutters. The recovered solution has been conditioned and analyzed like stream water samples. All trees sampled for this study are older than 100 years. Before drying, leaves and roots were treated during 15 min in an ultrasonic bath with distilled water in order to remove atmospheric dust and soil particles. The bark material has not been washed in order to get information about the atmospheric isotopic composition. Clean powder samples from trunks and branches were obtained with an ultraclean Ti-drill. All tree samples were dried at 80 °C during 24 h. Afterwards, 100–500 mg were completely digested in savillex vials using hot HNO₃ and H₂O₂. The REE concentrations of trees, soil leachates and waters were measured by inductively coupled plasma mass spectrometry (ICP-MS) in Strasbourg (Aubert et al., 2001) and Neuchâtel. The error of measurement is <5%. Standard techniques were applied for Sr and Nd isotopic analyses (Steinmann and Stille, 1997) and it was possible to run some of the beech samples. However, bad emissions on the mass spectrometer prevented precise Sr and Nd isotope

determinations on conifers. The Sr isotopic compositions were determined using a fully automatic VG Sector thermal ionization mass spectrometer at CNRS Strasbourg with a 5-cup multicollector after enrichment and separation from the bulk sample using cation exchange resin. During the measuring period the NBS 987 Sr standard yielded $^{87}\text{Sr}/^{86}\text{Sr} = 0.710258 \pm 5$ ($\pm\text{SD}$, $n = 9$). The Nd isotopic composition were determined using a Nu instruments MC-ICP-MS at the branch of Isotope Geology at the University of Bern. The in house standard yielded $^{143}\text{Nd}/^{144}\text{Nd} = 0.51105 \pm 1$ ($\pm\text{SD}$, $n = 7$) corresponding to the La Jolla Standard value of 0.511843.

4. Results and discussion

4.1. REE and Sr–Nd isotope signatures of Strengbach waters in the uppermost catchment

In a previous study, it has been shown that the Strengbach waters close to the source have Sr and Nd isotopic compositions very similar to values of primary apatite from

the granitic bedrock and the overlaying soil (Aubert et al., 2001; Table 1; Fig. 2). However, stream water normalized to apatite is still depleted in LREE pointing to an additional LREE depletion after apatite dissolution in the soil as expressed by a apatite normalized La_N/Yb_N ratio of <1 (Table 2; Fig. 3).

The pH of Strengbach water rises from 6.2 upstream (in the uppermost catchment) to 8.1 downstream (in the Rhine valley; Table 2). At the same time the major element composition of stream water (Table 3) evolves from Ca–Na– SO_4 type water upstream to Na–Ca–Cl– SO_4 – HCO_3 type

water downstream. Nevertheless, the evolution of pH and major element chemistry appear to have no direct impact on the REE distribution patterns which remain almost unchanged from upstream to downstream.

The DOC concentrations (Table 3) and La_N/Yb_N ratios (apatite normalized) (Table 2) of the uppermost catchment site (3999, 4015, 4109) are low, vary weakly and range between 1.2 and 1.4 mg/L and 0.12 and 0.22, respectively.

Leaching experiments performed on suspended load samples and bottom sediments of the Strengbach and on soil samples from a soil profile (0–50 cm depth) located in the water saturated zone close to the catchment outlet (ZS; Fig. 1) show that surface adsorption might be one of the mechanisms responsible for the observed additional depletion of the LREE (Fig. 4).

The Sr and Nd isotopic compositions of a 1 M HCl leachate of a $>0.45 \mu m$ suspended load sample from the catchment are comparable to those of the Strengbach stream water (Tricca et al., 1999). Similarly, 1 M HCl leachates from the lower part of a soil profile (20–50 cm) in the water saturated zone (ZS; Fig. 1; 510L2 and 512L2; Table 1) have stream water-like Sr and Nd isotopic compositions (triangle, #2 and 3 in Fig. 2). This indicates that leachable Sr and Nd adsorbed on the suspended load and soil minerals originate from surface water.

The REE patterns of the leached soil samples are the most LREE enriched with respect to stream water (Fig. 4) with stream water normalized La_N/Yb_N ratios of 2.2–2.7 (Table 4). The leachates of the suspended load samples have similar REE patterns with stream water normalized La_N/Yb_N ratios close to 2 (Fig. 4, Table 4), whereas the stream water normalized La_N/Yb_N ratios of bottom sediment leachates range between 1.8 and 1.9. Consequently, adsorption on suspended particles, bottom sediment and soil minerals might to some extent be responsible for the LREE depletion of stream water. However, the leachates of all sample categories remain LREE depleted

Table 1
Sr and Nd isotope data

Sample	Depth	$^{87}Sr/^{86}Sr$	$^{143}Nd/^{144}Nd$
Soil-508L2 (HCl leach.)	0–10 cm	0.72805(1)	0.51215(1)
Soil-510L2 (HCl leach.)	20–30 cm	0.72872(3)	0.51221(1)
Soil-512L2 (HCl leach.)	40–50 cm	0.73044(3)	0.51223(2)
508P (roots, <1 mm)	#2/0–10 cm #4/20–30 cm	0.72458(3)	0.51218(8)
510P (roots, <1 mm)		0.72974(1)	0.51211(1)
136 (bark wood; beech)		0.7251(5)	0.51212(4)
LP2 (leaves; beech)		0.72753(2)	0.51225(7)
LP19 (branch wood; beech)		0.72586(3)	0.51209(5)
PRH (roots wood; beech)		0.7336(2)	0.51217(3)
Lichen		0.71887(5)	0.51205(1)
Throughfall(a)		0.71857 ^a	0.51212(5)
Rainwater(b)		0.711–0.7146	n.d.
Soil solution(a)		0.72289(5)	0.51218(5)
Spring water(c)		0.72606(2)	0.51224(4)
Stream water(c)		0.72481(3)	0.51224(1)
Stream water 2(d)		0.72447(1)	0.51226(1)
Suspended load leach(d)		0.72023(5)	0.51224(1)
Apatite(a)		0.71612(1)	0.51228(1)

The errors given for the Sr and Nd isotopic compositions are two sigma mean values and refer to the last digits (values in parentheses). n.d., not determined.

(a) Aubert et al. (2002a,b); (b) Chabaux et al. (2005); (c) Aubert et al. (2001); (d) Tricca et al. (1999).

^a Three samples.

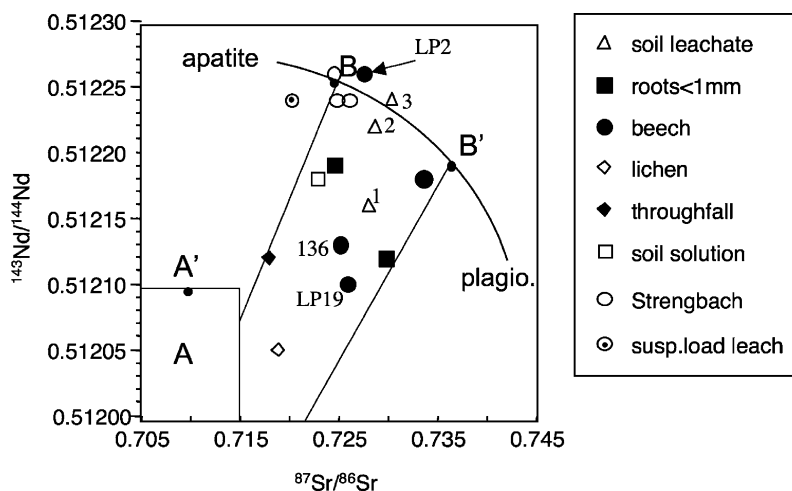


Fig. 2. Comparison of Sr and Nd isotope data of soil leachates and beech samples with Strengbach waters. Data of suspended load leachates, soil solution and stream waters from Aubert et al. (2001) and Tricca et al. (1999). A: atmospheric pool. B–B': range of Sr and Nd isotopic compositions of the alteration component taken up by the trees. All samples are from the uppermost Strengbach catchment. Most of the samples contain an atmospheric component A. Open triangle: soil leachates from ZS profile (depth: #1, 0–10 cm; #2, 20–30 cm; #3, 40–50 cm).

Table 2
REE concentration data of Strengbach waters, river Rhine and groundwater (nmol/L); distance in km from upper catchment^a

Samples	Dist. from catchment	La	Ce	Pr	Nd	Sm	Eu	Gd	Tb	Dy	Ho	Er	Tm	Yb	Lu	LaN/YbN apatite
3999	up.catchm.	0.06	0.13	0.03	0.17	0.07	0.01	0.08	0.01	0.08	0.01	0.04	n.d.	0.05	0.01	0.12
4015 ^b	up.catchm.	0.11	0.21	0.05	0.29	0.13	0.02	0.15	0.03	0.14	0.03	0.07	n.d.	0.04	0.01	0.22
4109	up.catchm.	0.12	0.28	0.06	0.39	0.15	0.03	0.18	0.03	0.17	0.03	0.07	n.d.	0.06	0.01	0.17
4108	1.5 km	0.15	0.24	0.05	0.28	0.11	0.02	0.13	0.02	0.14	0.03	0.07	n.d.	0.08	0.01	0.19
4016	2 km	0.09	0.11	0.03	0.15	0.05	0.02	0.06	0.01	0.07	0.02	0.04	n.d.	0.03	0.01	0.24
4112	3 km	0.08	0.14	0.03	0.18	0.07	0.01	0.08	0.01	0.09	0.02	0.05	n.d.	0.06	0.01	0.11
4017	5 km	0.14	0.15	0.04	0.20	0.07	0.01	0.08	0.01	0.08	0.02	0.05	n.d.	0.05	0.01	0.26
4019	5.5 km	0.09	0.10	0.03	0.15	0.05	0.01	0.06	0.01	0.05	0.01	0.02	n.d.	0.01	0.00	0.73
4020	7.5 km	0.11	0.15	0.03	0.18	0.06	0.01	0.08	0.01	0.07	0.02	0.05	n.d.	0.06	0.01	0.16
4022	14 km	0.09	0.11	0.02	0.10	0.03	0.01	0.05	0.01	0.05	0.01	0.04	n.d.	0.07	0.01	0.11

n.d.: not determined.

^a Data from Tricca et al. (1999).

^b Used for normalization.

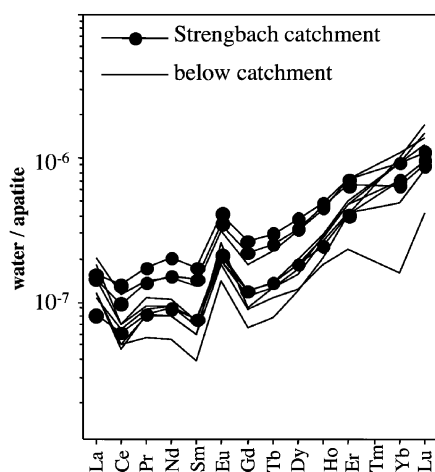


Fig. 3. Strengbach waters from the uppermost catchment (observatory) and from below the observatory normalized to apatite (Table 4).

when normalized to apatite demonstrating that LREE adsorption alone cannot explain the observed LREE depletion of stream water. All leachates show a positive stream water normalized Ce anomaly (Sholkovitz, 1993) ranging between +1.2 and 2.2 (Table 4) indicating that suspended load and soil particles are also sites for the oxidation of Ce (III) to Ce (IV).

Table 3
Major cations and anions of Strengbach water; distance in km from upper catchment^a

Sample	3999 up. catchm.	4015 up. catchm.	4109 up. catchm.	4108 1.5 km	4016 2 km	4112 3 km	4017 5 km	4019 5.5 km	4020 7.5 km	4022 14 km
Na ⁺ (mmol/L)	0.091	0.095	0.087	0.247	0.22	0.264	0.256	0.23	0.252	1.1
Mg ²⁺ (mmol/L)	0.028	0.029	0.025	0.03	0.11	0.038	0.109	0.139	0.126	0.201
K ⁺ (mmol/L)	0.023	0.022	0.016	0.04	0.044	0.048	0.043	0.048	0.044	0.133
Ca ²⁺ (mmol/L)	0.083	0.087	0.076	0.106	0.185	0.116	0.201	0.246	0.244	0.473
HCO ₃ ⁻ (mmol/L)	0.034	0.005	0.027	0.133	0.331	0.17	0.332	0.469	0.437	1.12
NO ₃ ⁻ (mmol/L)	0.049	0.051	0.029	0.036	0.057	0.048	0.06	0.069	0.068	0.082
SO ₄ ²⁻ (mmol/L)	0.093	0.099	0.094	0.089	0.097	0.093	0.107	0.112	0.118	0.346
Cl ⁻ (mmol/L)	0.061	0.079	0.06	0.175	0.235	0.195	0.259	0.226	0.245	0.629
Σ cations (meq/L)	0.336	0.349	0.305	0.559	0.854	0.620	0.919	1.05	1.04	2.58
Σ anions (meq/L)	0.330	0.333	0.304	0.522	0.817	0.599	0.865	0.99	0.99	2.52
DOC (mg/L)	1.27	1.23	1.44	2.05	1.43	2.77	1.60	1.79	1.88	3.31
pH	6.2	6.4	6.2	6.8	7.4	7.3	7.4	7.6	7.5	8.1

^a Tricca (1997).

4.2. The Sr–Nd isotope signatures of vegetation

Fig. 2 shows Nd and Sr isotopic compositions of the Strengbach waters from the uppermost catchment together

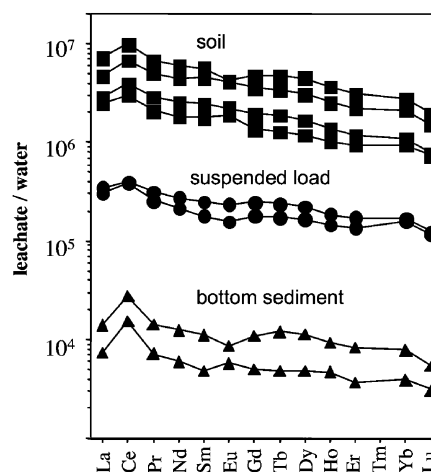


Fig. 4. REE of soil (from ZS profile), suspended load and bottom sediment leachates normalized to stream water (4015, Table 2). Suspended load and bottom sediment of the Strengbach are taken in the uppermost catchment. All samples are LREE enriched compared to Strengbach waters and have a positive Ce anomaly.

Table 4
REE concentrations of soil, bottom sediment and suspended load leachates (ppm)

Samples	La	Ce	Pr	Nd	Sm	Eu	Gd	Tb	Dy	Ho	Er	Tm	Yb	Lu	La/Yb norm.	Ce/Ce* norm.
Soil 508L2	37.0	87.7	14.6	75.7	34.0	6.6	32.6	5.4	27.2	4.4	10.4	1.2	7.3	1.0	2.59	1.35
Soil 510L2	43.8	115.2	20.1	106.1	47.2	7.8	46.5	7.9	38.3	5.9	13.0	1.5	8.3	1.0	2.69	1.42
Soil 512L2	70.6	196.3	35.2	188.8	86.3	14.2	86.4	14.3	70.7	10.9	24.5	2.8	16.2	2.0	2.24	1.46
Soil 515L2	108.3	285.2	47.2	251.0	108.2	14.8	113.1	20.1	103.4	15.6	34.1	3.9	21.6	2.6	2.58	1.45
Susp. load 4109/32 ^b	5.2	11.6	2.2	11.5	4.8	0.82	5.9	1	5.1	0.8	1.9	0.23	1.3	0.16	2.05	1.24
Susp. load 4108/33 ^b	4.6	11.3	1.8	9	3.4	0.55	4.3	0.7	3.8	0.63	1.5	0.19	1.2	0.15	1.97	1.41
Bottom sedi. 4109/32 ^b	0.21	0.79	0.1	0.52	0.21	0.03	0.26	0.05	0.26	0.04	0.09	0.01	0.06	0.007	1.8	2.02
Bottom sedi. 4108/33 ^b	0.11	0.44	0.05	0.25	0.09	0.02	0.12	0.02	0.11	0.02	0.04	0.01	0.03	0.004	1.88	2.21
Apatite ^a	103.3	298.1	51.2	276.8	132.8	10.0	109.1	16.8	71.4	9.4	16.9	2.3	11.9	1.5		

La/Yb and Ce/Ce*: water normalized (see Table 2).

^a Aubert et al. (2002a,b).

^b Tricca et al. (1999).

with a calculated mixing curve defined by the end-members apatite and plagioclase extracted from local bedrock (mixing curve of alteration products; Aubert et al., 2001). All other bedrock and soil minerals plot far off this mixing curve towards more radiogenic Sr isotope ratios outside the range of Fig. 2 (Aubert, 2001; Aubert et al., 2001). Thus, there is no soil sample or mineral plotting to the left of this mixing curve. However, atmospheric precipitations which are additional Sr and Nd sources for the Strengbach catchment have low $^{143}\text{Nd}/^{144}\text{Nd}$ and $^{87}\text{Sr}/^{86}\text{Sr}$ ratios and plot to the left of the mixing curve. Their Nd–Sr isotopic compositions have been deduced from eolian particles and rain water plotting to the lower left of the diagram (A, Fig. 2) (Aubert et al., 2002b). Lichens, whose nutrients are known to derive largely from airborne particulate matter (e.g., Rossbach et al., 1999) have been sampled at the surface of tree barks and analyzed for Sr and Nd isotopes (Table 1). Their $^{87}\text{Sr}/^{86}\text{Sr}$ ratio is 0.71887 and similar to that of throughfall (0.71857, Table 1) and slightly higher than rainwater values that vary between 0.711 and 0.7146 (Chabaux et al., 2005). The $^{143}\text{Nd}/^{144}\text{Nd}$ ratio is only slightly different for lichens and throughfall (0.51205 and 0.51212, respectively). Therefore, soil samples, soil solutions or trees plotting to the lower left of the mixing curve for alteration products suffered atmospheric contamination.

Only one of the beech samples (LP2, young leaves) has Sr and Nd isotopic compositions (0.7275 and 0.51225, respectively) which are close to those of surface waters (average: 0.725 and 0.51225, respectively). Its isotopic composition is close to the alteration component taken up by the tree and defined in Fig. 2 as point B and composed by 15 wt% of apatite and 85 wt% of plagioclase (Aubert et al., 2001).

The two root samples (<1 mm) shown in Fig. 2 originate from the ZS soil profile discussed in Section 4.1 (Table 1; 508P, 510P). Their Sr and Nd isotopic composition values are shifted towards atmospheric composition and plot close to soil solution and to the topsoil leachate (triangle #1 in Fig. 2; ZS 508L2; 0–10 cm depth; Table 1). Similar

$^{87}\text{Sr}/^{86}\text{Sr}$ isotopic composition values ranging between 0.725 and 0.734 have also been found in four beech samples (roots, bark, branches and leaves). Their $^{143}\text{Nd}/^{144}\text{Nd}$ isotopic composition values vary between 0.51209 and 0.51225. The bark (#136) and the wood of a beech (LP19; branch) contain important quantities of atmospheric Sr and Nd as indicated by their low $^{87}\text{Sr}/^{86}\text{Sr}$ and $^{143}\text{Nd}/^{144}\text{Nd}$ ratios.

The throughfall and lichen samples plot closest to A (Aubert et al., 2002b; A', 0.71 and 0.5121, respectively). Using these atmospheric end-member isotopic compositions and an alteration component B' on the mixing curve of alteration products (containing 5 wt% of apatite and 95 wt% of plagioclase; corresponding to $^{87}\text{Sr}/^{86}\text{Sr}$ and $^{143}\text{Nd}/^{144}\text{Nd}$ values of 0.735 and 0.51219, respectively; for more details see model of Aubert et al., 2001), one can deduce that throughfall contains up to 50% and soil solution more than 20% of atmospheric Sr and Nd (Aubert et al., 2002b). Similarly, high atmospheric contributions can be estimated for the beech samples with lowest Sr and Nd isotopic compositions closely situated to throughfall and lichen samples (#136, LP19; Table 1). The estimation of the atmospheric contribution remains very approximative because the isotopic composition of the atmospheric component is not yet precisely known. The new data from the beech (#136, LP19) and lichen samples point to a Nd isotopic composition for the atmospheric component that is even lower than that of point A' in Fig. 2. If some of the bark contained detrital REE of the soil, then the atmospheric contribution would even be higher than estimated because all soil minerals have much higher $^{87}\text{Sr}/^{86}\text{Sr}$ isotopic ratios than the atmospheric component and plot to the right of the mixing curve in Fig. 2.

4.3. The LREE uptake by vegetation

The trees REE concentrations (Table 5) were normalized to Strengbach water sampled close to its source (sample 4015, Table 2) (Fig. 5a) because tree samples without atmospheric contribution (e.g., LP2; Table 1) carry

Table 5
REE concentrations in plants (ppb)

Sample	La	Ce	Pr	Nd	Sm	Eu	Gd	Tb	Dy	Ho	Er	Tm	Yb	Lu	SREE	Eu/Eu ^a	La/Yb ^a	La/Yb ^b	La/Yb ^c	La/Yb ^d	Eu/Eu ^d
LP2/leaves, beech ^c	65	62	7	25	4	3	5	1	3	1	2	0.2	1	0.3	178	3.7	31	7	12.1	54	6
LP16/bark, beech ^c	26	38	5	18	4	17	4	n.d.	2	1	2	0.3	1	0.3	118	27.9	17	4	5.8	26	54
LP19/branch, beech ^c	51	62	7	27	5	12	7	1	3	1	2	0.3	1	0.2	179	12.2	20	4	7.0	31	23
P22/bark, beech ^c	75	163	19	70	14	5	14	2	8	2	4	0.5	3	0.4	380	2.2	14	3	4.3	19	3
LP25/roots, beech, 1 mm ^c	190	411	49	182	40	16	39	5	25	4	11	1.5	8	1.4	984	2.4	12	3	3.4	15	4
LP26/roots, beech, 5–8 mm ^c	26	54	6	23	5	8	6	1	3	1	1	0.2	1	0.2	136	9.4	12	3	3.5	16	18
PRH roots, beech ^c	986	2039	245	878	173	33	160	19	82	14	39	4.6	31	4.5	4707	1.2	17	4	5.6	25	1
RIH/roots, beech ^c	279	603	69	248	49	13	48	6	28	5	12	1.7	12	1.6	1375	1.6	12	3	3.8	17	2
508P/roots<1 mm ^c	63	129	19	82	28	5	24	4	18	3	7	1	6	0.9	389	1.2	6	1	0.9	4	1
510P/roots<1 mm ^c	1718	3805	539	2490	815	116	718	109	527	79	178	21	123	15	11,254	0.9	7	2	1.5	6	0.5
512P/roots<1 mm ^c	2270	5320	817	4037	1485	219	1350	213	1047	159	362	43	252	31	17,606	0.9	5	1	0.3	1	0.6
515P/roots<1 mm ^c	4781	11278	1668	7846	2728	352	2493	392	1884	284	640	76	448	55	34,925	0.8	5	1	0.7	3	0.3
A5: bark, beech ^c	243	127	66	249	51	16	43	9	32	8	16	4	12	4	880	2.1	10	2	2.9	13	3
F1/stem, beech ^f	71	158	22	75	13	19	14	3	13	3	7	2	7	1	408	8.6	5			3	16
F2/stem, beech ^f	28	74	8	24	4	4	3	n.d.	2	n.d.	n.d.	n.d.	1	n.d.	148	7.0	14			21	13
F206/leaves, beech ^f	265	490	55	195	37	16	39	8	26	7	12	4	9	4	1167	2.6	15			22	4
F4/stem, conifer ^f	34	80	11	35	9	8	10	2	6	1	3	1	3	1.0	204	5.1	6			4	9
H2/stem, conifer ^f	27	53	6	19	5	2	3	n.d.	4	1	2	n.d.	1	n.d.	123	3.2	14			20	5
15/bark, limetree ^g	728	1650	198	851	194	48	227	34	194	37	104	15	89	13	4382	1.4	4			1	2
16/stem, limetree ^g	33	58	10	37	8	3	5	1	6	2	3	1	2	2	171	2.9	8			9	5
P6/bark, limetree ^g	506	931	130	470	83	20	88	11	70	13	37	5	30	4	2398	1.4	9			9	2
P7/stem, limetree ^g	19	21	4	13	3	3	2	n.d.	2	n.d.	1	n.d.	n.d.	n.d.	68	7.5					14
P1/bark, beech ^g	404	779	102	376	73	18	69	11	55	10	27	5	22	4	1955	1.5	9			11	2
A8/lichen ^c	184	354	42	166	36	7	29	4	22	5	13	2	12	2	878	1.3	8	1.8			

n.d., not detected.

^a Strensbach-norm. (in Table 2).

^b Apatite norm.

^c Apatite norm. and atmos. correct. (50%).

^d Strensbach-norm. and atmos. correction (50% contr.): $2 * ((La_N/Yb_N)_{plant}) - (La_N/Yb_N)_{lichen}$; $2 * (Eu/Eu^*_{plant}) - (Eu/Eu^*_{lichen})$.

^e Strensbach catch.

^f Black Forest.

^g Strasbourg.

essentially the isotopic signature of stream water. The trees are strongly REE enriched with respect to stream water. Most enriched (up to 100,000 times) are small roots with 1–2 mm in diameter. Larger roots are up to 1000 times en-

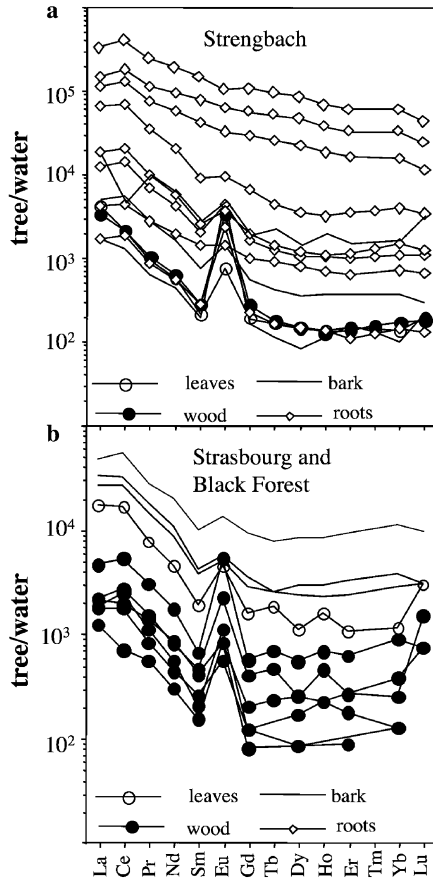


Fig. 5. Plant samples from the Strengbach catchment [Vosges Mountains (a)] and Strasbourg and Black Forest (b) normalized to the REE composition of the filtered stream water (sample 4015; Table 2). Wood stands for trunk and branch.

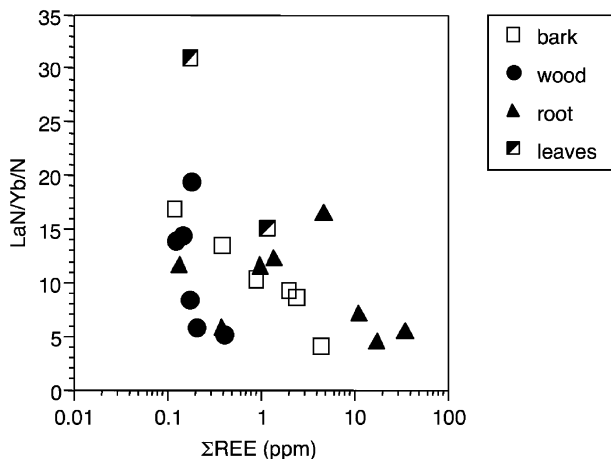


Fig. 6. La/Yb ratios in plants normalized to the REE composition of the filtered stream water (sample 4015; Table 2) and compared with the total REEs. Wood stands for trunk and branch.

riched. Wood and bark of branches and trunks have lower REE concentrations with a strong positive Eu anomaly (Fig. 5). Furthermore, a strong LREE enrichment can be observed in some of the tree samples (Fig. 6). Normalized to Strengbach water, these samples show La_N/Yb_N ratios ranging between 5 and 30. The smallest roots (508P, 510P, 512P, 515P; Table 5) are least LREE enriched with lowest La_N/Yb_N ratios between 5 and 7.

The stream water normalized Eu anomalies and La_N/Yb_N ratios given in Table 5 have been corrected for atmospheric contamination using the REE distribution pattern of a lichen sample (see Table 5 for calculation details). The atmosphere corrected Eu anomalies and La/Yb ratios are generally higher than the uncorrected ones because the Eu anomaly (1.3 when normalized to stream water) and the La_N/Yb_N ratios of lichen (8 when normalized to stream water) are lower than for most vegetation samples (Table 5). Trees from outside the catchment from the city of Strasbourg in the Rhine valley further to the North and in the Black Forest on the other side of the Rhine Valley show very similar REE patterns (Fig. 5b) indicating that this kind of fractionation with LREE- and Eu-enrichment is not a local phenomenon.

The distribution patterns of plants normalized to apatite (Fig. 7), which is the most important REE source for plants and waters as shown by the Sr and Nd isotope data (Fig. 2), point to LREE enrichments with atmosphere corrected La_N/Yb_N ratios equal or lower than 12 (Table 5). The apatite normalized REE distribution patterns of the smallest roots are least fractionated and emphasize the idea, that most of the REE in the plants of the Strengbach catchment originate from apatite dissolution. Plant roots are known to attack specifically apatite, an important phosphate source for plant growth (Wallander et al., 1997). Upward in the tree, REE concentrations decrease in trunk, bark and leaves, simultaneously with the appearance of a strong positive Eu anomaly and a strong LREE enrichment (Figs. 6 and 8).

This general evolution suggests that REE fractionation is controlled by metabolic processes within the plant rather than by preferential uptake of LREE and Eu at the root-soil interface, e.g., due to bacterial activity, because major fractionation occurs within the plant and not at the soil-plant interface. This is in agreement with earlier observations indicating that the roots fractionate the REE during uptake from soil solution much less than other parts of the plant during transport and deposition within stem and leaves (Li et al., 1998; Bei Wen et al., 2001; Zhang et al., 2002). However, similar to our study (e.g., Fig. 6) it has also been observed that the root is the most REE-enriched part of the plant and that roots of rice and wheat have always lower La/Yb ratios than corresponding leaves (e.g., Bei Wen et al., 2001). Recent studies indicate that rare earth elements have a dual effect on the physiological and biochemical reactions in the plant development (Zeng et al., 2003 and citations therein). Important resemblances exist between Eu^{3+} and Ca^{2+} in their atomic radius and

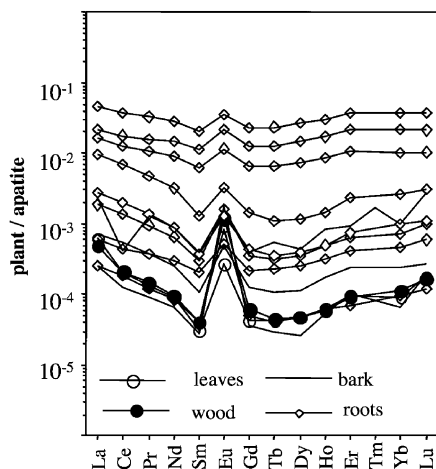


Fig. 7. REE of plant samples from the Strengbach catchment normalized to apatite (Table 4). Wood stands for trunk and branch.

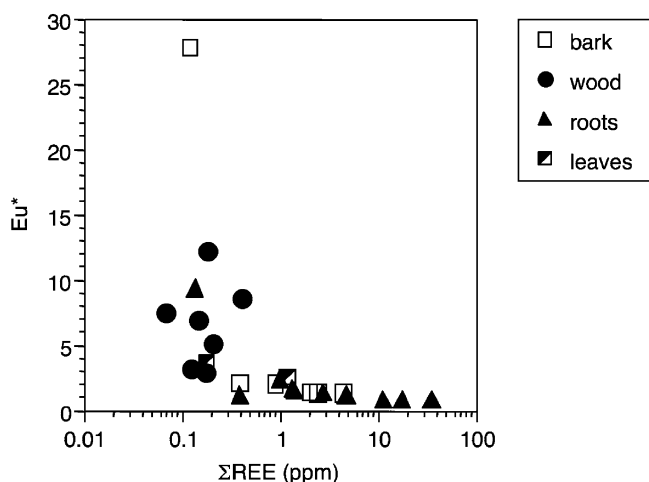


Fig. 8. Eu anomaly in plants as a function of total REEs. Wood stands for trunk and branch.

structures of the valence electron and Zeng et al. showed that Eu^{3+} might replace Ca^{2+} in plants (e.g., *Amaranthus caudatus*) and promote calcium transportation across plasma membrane. Thus, possibly some of the trees Ca, which plays a vital role in the formation and the stabilization of the plants cellular walls, in the stabilization of membranes and in the regulation of the intracellular metabolism, might have been replaced by Eu^{3+} . The concentration of free and active Ca^{2+} in the cytoplasm of plant cell must remain low and is controlled by the precipitation of oxalate crystals which allows the storing of inactive Ca and probably also of Eu in the old plant organs.

More than 99% of the dry mass of a beech or a spruce corresponds to branches, stem, coarse roots (>2 mm) and leaves. The smallest roots (<2 mm) represent less than 0.5% of the whole tree mass (Scarascia-Mugnozza et al., 2000). Therefore, the REE pattern of the bulk tree reflects the REE distribution of bark, trunk and leaves, i.e., characterized by a strong LREE enrichment and a positive

Eu anomaly (stream water normalized). The weaker LREE enrichment (stream water normalized) of the small roots completely disappears in this total budget in spite of their elevated REE concentrations. Consequently, our data clearly demonstrate that vegetation preferentially accumulates LREE and Eu. Vegetation thus represents an important sink for LREE in forested catchments. In the following section we will discuss how preferential accumulation of LREE by vegetation might modify the REE budget at catchment scale.

4.4. The impact of vegetation on the REE budget of the Strengbach catchment

The REE of soil and soil solutions of a small catchment might be exported by draining waters and/or vegetation. Both of them, the annual flow rate of the Strengbach at the outlet and the annual growth rate of vegetation are known. Based on long-term monitoring an average discharge rate of 20 L/s can be deduced (Probst and Viville, 1999). However, during dry years the mean flow rate can be as low as 9 L/s (Probst et al., 1995; Aubert et al., 2002a). The average discharge rate of 20 L/s leads to an annual dissolved LREE (La–Nd) and HREE (Er–Lu) export of 0.248 mol (35 g) to 0.532 mol (76 g) for LREE and 0.061 mol (10 g) to 0.091 mol (16 g) for HREE. The source data for this calculation are given in Table 6.

For the vegetation of the Strengbach catchment an average growth rate of $7 \text{ m}^3/\text{ha}/\text{year}$ has been determined (Prevosto, 1988). Taking this value and 80 ha for the catchment surface and the additional parameters given in Table 6, one can calculate that vegetation extracts at least 0.319 mol (45 g) of LREE and 0.009 mol (1.5 g) of HREE per year. These values are deduced from tree samples whose average LREE and HREE concentrations are $0.952 \text{ nmol g}^{-1}$ (0.135 ppm) and $0.027 \text{ nmol g}^{-1}$ (0.005 ppm), respectively. These concentrations include correction for weight loss due to drying and for atmospheric contribution. Using tree samples including larger roots, a LREE and HREE export of 0.816 mol (114 g) and 0.018 mol (2.7 g), respectively, can be calculated. All samples (except the smallest roots representing less than 0.5% of the whole tree mass) can be used to calculate similar export values for LREE and HREE of 131 and 4 g, respectively. These results are only semi-quantitative because parameters such as wood density and water content used for this estimation are variable. Nevertheless they clearly indicate that the yearly LREE uptake by vegetation is comparable with the yearly LREE export by the streamlet. It appears that the LREE export by vegetation can even be higher than that of stream discharge. However, the HREE discharge by the Strengbach stream with 0.076 mol (13 g) in average and with extreme values of 0.061 mol (10 g) to 0.091 mol (16 g) is always more important than the uptake by plants (Table 6, Fig. 9).

Table 6
Flux parameters for REE

(a) Strengbach (catchment)
Samples 3999, 4015, 4109; (Table 2):
Concentrations:

	Average		Low		High	
	ng/L	nmol/L	ng/L	nmol/L	ng/L	nmol/L
LREE (La–Nd)	89	0.618	56	0.393	120	0.843
HREE (Er–Lu)	20	0.121	17	0.097	25	0.145
Average annual discharge: 20 L/s						
	g	mol	g	mol	g	mol
Export LREE:	56	0.390	35	0.248	76	0.532
Export HREE:	13	0.076	10	0.061	16	0.091

(b) Vegetation (catchment)
catchment surface:
Growth rate of vegetation:

80 ha
7 m³/ha/a
560 m³/a
0.6 kg/dm³

Wood density:

<http://www.worldagroforestry.org/sea/Products/AFDbases/WD/Index.htm>

(A) samples (catchment) without roots LP2, LP16, LP19, P22, LP25, LP26, A5:

(B) with roots (catchment; except the smallest samples 508P–515P)

(C) all samples (including those from outside the catchment, except 508P–515P)

	A		B		C	
	µg/g	nmol/g	µg/g	nmol/g	µg/g	nmol/g
LREE in dried sample:	0.34	2.379	0.855	6.073	0.88	6.258
HREE in dried sample:	0.011	0.066	0.02	0.135	0.03	0.202
25% wt loss during drying						
LREE in wet sample:	0.27	1.903	0.68	4.858	0.70	5.006
HREE in wet sample:	0.009	0.053	0.016	0.108	0.024	0.161
50% atmospheric origin						
LREE in vegetation:	0.135	0.952	0.34	2.429	0.35	2.503
HREE in vegetation:	0.0045	0.027	0.008	0.054	0.012	0.081
	g	mol	g	mol	g	mol
Export LREE:	45	0.319	114	0.816	118	0.841
Export HREE:	1.5	0.009	2.7	0.018	4	0.027

4.5. The fate of vegetation hosted REE after degradation

The results of the budget calculations presented in Section 4.4 demonstrate that LREE uptake by vegetation can explain the observed LREE depletion of stream water. Fig. 9 also implies that degradation of LREE-enriched plant tissue should lead to the formation of a LREE-enriched litter layer in the topsoil which, however, is not confirmed by our data. Consequently, there must be a process that exports these LREE from the catchment. Some of the LREE in the litter layer may also directly be recycled and re-absorbed by vegetation. However, the fact that the roots show compared to other parts of the plant only a relatively weak LREE enrichment suggests that this recycling does not significantly influence the REE budget at catchment scale. If LREE recycling would play an important role one might suggest that older plants are more LREE enriched than younger plants. This however is not the case. We found similar La/Yb ratios in adult trees and in only 30 days old corn plants.

In previous studies, it has been shown that two principal pools for REE in 0.22 or 0.45 µm-filtered river water exist:

a REE-rich colloidal pool with shale-like distribution patterns and a dissolved pool with HREE enrichment (Elderfield et al., 1990). Thus, the presence of different quantities of colloidal phases in the <0.45 µm fraction may explain the variable degree of LREE depletion of the different samples. A more recent study on the boreal Kalix river confirms that colloidal particles dominate the transport of filter-passing REE and that the colloidal fraction shows a flat to slightly LREE-enriched pattern, whereas the “truly” dissolved <3 kDa fraction shows HREE-enriched patterns with respect to bedrock (Ingri et al., 2000). However, this study also indicates that the REE in the colloidal and particulate fraction are associated with an organic-rich and Fe-rich inorganic phase. The authors further show that La concentrations are positively correlated with dissolved organic carbon (DOC) and water discharge. Especially during flood events (e.g., in spring) when the river has a large exchange surface with vegetation, woodland and soil, DOC and La concentrations are high. Similarly, the study on river waters from a small catchment in the Cameroon shows that the Mengong river with DOC contents of up to 24 mg/L has much higher

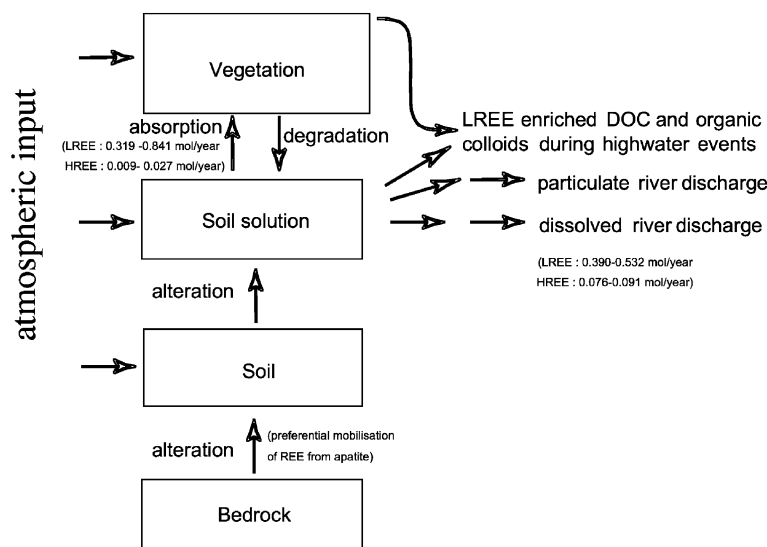


Fig. 9. Flux boxmodel for LREE and HREE at the atmosphere–water–soil–plant interface. The yearly LREE uptake by vegetation is comparable with the yearly LREE export by the streamlet. LREE export from catchment basins with DOC during high water events might be the process that counterbalances plant-derived LREE accumulation in the litter layer of the topsoil.

La_N/Yb_N ratios (0.8; PAAS norm) than the Nyong river with DOC contents of up to 14 mg/L (0.5; PAAS norm; Viers et al., 1997). These examples demonstrate that increasing DOC contents correlate with LREE enrichments in waters, which is in agreement with the concept that DOC in river water is mainly derived from decomposition of plant tissue. Consequently, LREE export from catchment basins with DOC during high water events might be the process that counterbalances plant-derived LREE accumulation in the litter layer of the topsoil. LREE and DOC export seems to occur mainly during high water events, whereas normal river discharge is characterized by LREE-depleted patterns inherited from soil water.

However, REE in organic-rich blackwaters (filtered at 0.45 µm) of the Great Dismal Swamp (Virginia) behave differently and are all enriched in the middle REEs when normalized to upper continental crust and not in the LREE as suggested in our case (Johannesson et al., 2004). Johannesson et al. show that organic complexes are the predominant form for dissolved REE despite significant competition with Fe and Al. One possible explanation for this different behavior might be the fact that these relatively quiet lake and swamp waters contain comparatively small quantities of organic-rich suspended particles. Therefore, the MREE-enriched organic complexes of the Great Dismal Swamp might be issued from solution complexation under hydrodynamically quiet conditions with little or no suspended particles, whereas rivers and streams drain, especially after flood events, suspended organic- and LREE-rich particulates and colloidal phases.

Unfortunately in the case of the Strengbach catchment no REE water data are available for flood events. However, previous uranium isotope studies in the catchment have shown that during flood events parts of U are supplied by superficial horizons of soils, probably complexed

by organic colloids or adsorbed on organic particles (Riotte and Chabaux, 1999). DOC and U contents increase significantly at the beginning of a storm event in the catchment and, particularly, the DOC behavior reflects the leaching of the upper soil layers enriched in organic matter (Soulsby, 1992, 1995; Ladouche et al., 2001). Similar to the existing Sr and U isotope data (Riotte and Chabaux, 1999; Ladouche et al., 2001; Aubert et al., 2002a,b) new Ca isotope data also suggest that chemical fluxes from the topsoil become more important with increasing discharge (Schmitt, 2003; Schmitt et al., 2003; Schmitt and Stille, 2005). This is indicated by the positive correlation between $\delta^{44}\text{Ca}$ values and discharge at the outlet of the Strengbach catchment. The high $\delta^{44}\text{Ca}$ corresponding to a high discharge rate has been explained by an enhanced contribution of soil water. Interstitial soil water is depleted in the light ^{40}Ca isotope due to biological activity in the topsoil. Plants are recognized to absorb preferentially the light ^{40}Ca isotope (Schmitt et al., 2003; Schmitt and Stille, 2005 and citations therein) leading to a ^{40}Ca depletion of soil water. All these data thus show, that important quantities of organic matter are extracted from the topsoil of the Strengbach catchment during high water events similar to the Kalix study of Ingri et al. (2000) that LREE-enriched small organic matter particles/colloids are exported from the Strengbach catchment during high water events preventing formation of LREE-enriched topsoil.

4.6. REE absorption by vegetation at a global scale

Until now the impact of vegetation on the distribution of dissolved REE has only been discussed at the scale of the Strengbach catchment. In the following this impact shall be considered on a geographically larger scale. At

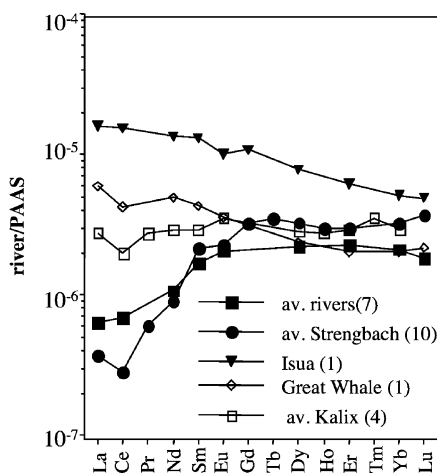


Fig. 10. PAAS normalized filtered 0.45–0.2 μm river water from different climate zones. For temperate and tropical zones: average rivers [7 samples: Mississippi, Ohio, Rhine, Pampanga, Shinano, Amazon, Indus (Goldstein and Jacobsen, 1988a,b; Tricca et al., 1999)] and average Strengbach (10 samples; Tricca et al., 1999). Boreal zone: Kalix river (4 samples; filtered $<0.2 \mu\text{m}$; their PAAS normalized La_N/Yb_N ratios range between 0.5 and 2; Ingri et al., 2000). Arctic zone: Lake Isua, Great Whale (Goldstein and Jacobsen, 1988a,b).

regional scale, bedrock lithology plays only a minor role in defining the REE chemistry of river water (Elderfield et al., 1990). In Fig. 10 are shown the PAAS (post-Archean Australian shales) normalized dissolved load REE patterns of the Strengbach (average value of 10 samples) and large rivers draining temperate and tropical regions (average value of Amazon, Indus, Mississippi, Ohio, Pampanga, Shinano, Rhine) together with data from boreal and arctic zones (Kalix river in northern Sweden, Great Whale in NW Quebec and lake Isua in Eastern Greenland) (Goldstein and Jacobsen, 1988a; Tricca et al., 1999; Ingri et al., 2000). The comparison shows that the small Strengbach streamlet has REE distribution patterns very similar to those of large rivers and that rivers draining temperate or tropical regions are more depleted in LREE than rivers from boreal and arctic zones. The PAAS normalized average La_N/Yb_N ratio of the Strengbach is 0.12 whereas the ratios of the tropical and temperate rivers range between 0.12 and 0.39. The Kalix river (filtered $<0.2 \mu\text{m}$), draining a boreal region in Northern Sweden (Ingri et al., 2000), shows PAAS normalized La_N/Yb_N ratios ranging between 0.5 and 2. Even more LREE enriched are water samples from arctic regions (Goldstein and Jacobsen, 1988a), with a La_N/Yb_N of 2.9 for Great Whale and 3.1 for lake Isua.

The LREE depletion which apparently tends to disappear at higher latitudes is probably either the result of the successive disappearance of vegetation, the important sink for LREE, or of the superposition of both effects, the disappearance of vegetation and the increasing importance of colloidal phases. At this point it is impossible to distinguish between the superposing effects of organic/inorganic colloid induced LREE enrichment and the decreasing effect of LREE depletion due to the disappearance of

vegetation. The only exceptions that do not follow this general trend are the Mengong river in Cameroon (Viers et al., 1997) with high DOC concentrations (25 mg/L) and the Kalix river (Ingri et al., 2000) during flood events. The Kalix river has high filtered La ($<0.45 \mu\text{m}$) and high dissolved organic carbon contents (0.7 μm) which can, as discussed in Section 4.5, be related to the presence of LREE-enriched organic colloids. $^{143}\text{Nd}/^{144}\text{Nd}$ ratios and $^{147}\text{Sm}/^{144}\text{Nd}$ ratios of the same Kalix river waters confirm the important influence of dissolved organic carbon on the REE composition of the 0.45 μm filtered water fraction (Öhlander et al., 2000; Andersson et al., 2001). These ratios are significantly lower than those of the average bedrock but show a closer resemblance with ratios found in humic and plant material.

Further studies shall help to answer these questions. Nevertheless, the Strengbach case study has shown that REE uptake by vegetation is besides apatite dissolution, complexation and lanthanide adsorption on colloids, suspended load and river ground sediments another important factor controlling the LREE fractionation in waters.

5. Summary and conclusions

Sr and Nd isotope data show that the dissolved REE of stream water mainly originate from dissolution of apatite during weathering. However, stream water REE patterns normalized to apatite are still depleted in light REE pointing to the presence of an additional LREE depleting process.

The leaching experiments performed on suspended load samples, bottom sediments of the Strengbach and on soil samples indicate that surface adsorption is one of the mechanisms responsible for the observed additional depletion of the LREE. It has also been shown that suspended load and soil particles are sites for the oxidation of Ce (III) to Ce (IV). Thus, due to adsorption processes some of the waters circulating in the soil are already additionally depleted in LREE and Ce before they enter the stream.

Vegetation might be another important factor controlling LREE depletion of river water. Vegetation samples are strongly enriched in LREE compared to surface and soil water and their Sr and Nd isotopic composition is after correction of the atmospheric contribution comparable with that of apatite and stream water. Mass balance calculations indicate that the yearly LREE uptake by vegetation is comparable with the LREE export by stream water.

The data further imply that degradation of LREE-enriched plant tissue should lead to the formation of a LREE-enriched litter layer in the topsoil. We suggest that this subsequent LREE enrichment is counterbalanced by LREE export from catchment basins together with DOC and small organic matter particles/colloids during high water events when the surface waters have a large exchange surface with vegetation and soil.

The LREE depletion is observable for nearly all large river systems. It apparently tends to disappear at higher

latitudes and is probably either the result of the successive disappearance of vegetation or due to the superposition of both effects, the disappearance of vegetation and the increasing importance of LREE-enriched colloidal phases.

Acknowledgments

We sincerely thank K. Johannesson, E. Sholkovitz and an anonymous reviewer for their constructive comments and R.H. Byrne for editorial handling. The hospitality at the branch of Isotope Geology of the University of Berne and the great help of Th. Nägler during the Nd isotope measurements on the MC-ICPMS is gratefully acknowledged. We also thank R. Boutin, J.-J. Frey, B. Kiefel and Th. Perrone of the Centre de Géochimie de la Surface at Strasbourg for their technical assistance and analytical work. This study has been financially supported by REALISE (REseau Alsace de Laboratoires en Ingénierie et Sciences pour l'Environnement) and the region of the Alsace. This is EOST contribution 2006.202-UMR7517.

Associate editor: Robert H. Byrne

References

- Akagi, T., Fu, F.F., Yabuki, S., 2002. Absence of Ce anomaly in the REE patterns of peat moss and peat grass in the Ozegahara peatland. *Geochem. J.* **36**, 113–118.
- Allègre, C.J., Dupré, B., Nègre, P., Gaillardet, J., 1996. Sr–Nd–Pb isotope systematics in Amazon and Congo river systems: constraints about erosion processes. *Chem. Geol.* **131**, 93–112.
- Amiotte-Suchet, P., Aubert, D., Probst, J.L., Gauthier-Lafaye, F., Probst, A., Viville, D., Andreux, F., 1999. $\delta^{13}\text{C}$ pattern of dissolved inorganic carbon in a small catchment: the Strengbach case study (Vosges mountains, France). *Chem. Geol.* **159**, 129–145.
- Andersson, P.S., Dahlgvist, R., Ingri, J., Gustafsson, Ö., 2001. The isotopic composition of Nd in a boreal river: a reflection of selective weathering and colloidal transport. *Geochim. Cosmochim. Acta* **65**, 521–527.
- Aubert, D., 2001. Contribution de l'altération et des apports atmosphériques aux transferts de matières en milieu silicaté: traçage par le strontium et les terres rares. Cas du bassin versant du Strengbach (Vosges, France). PhD Thesis, University of Strasbourg.
- Aubert, D., Stille, P., Probst, A., 2001. REE fractionation during granite weathering and removal by waters and suspended loads: Sr and Nd isotopic evidence. *Geochim. Cosmochim. Acta* **65**, 387–406.
- Aubert, D., Probst, A., Stille, P., Viville, D., 2002a. Evidence of hydrological control of Sr behavior in stream water (Strengbach catchment, Vosges mountains, France). *Appl. Geochem.* **17**, 285–300.
- Aubert, D., Stille, P., Probst, A., Gauthier-Lafaye, L., Pourcelot, L., DelNero, M., 2002b. Characterization and migration of atmospheric REE in soils and surface waters. *Geochim. Cosmochim. Acta* **66**, 3339–3350.
- Aubert, D., Probst, A., Stille, P., 2004. Distribution and origin of major and trace elements (particularly REE, U and Th) into labile and residual phases in an acid soil profile (Vosges Mountains, France). *Appl. Geochem.* **19**, 899–916.
- Wen, Bei, Yuan, Dong-an, Shan, Xiao-quan, Li, Fu-liiang, Zhang, Shu-zhen, 2001. The influence of rare earth element fertilizer application on the distribution and bioaccumulation of rare earth elements in plants under field conditions. *Chem. Spec. Bioavail.* **13**, 39–48.
- Blum, J.D., Erel, Y., Brown, K., 1994. $^{87}\text{Sr}/^{86}\text{Sr}$ ratios of Sierra Nevada stream waters: implications for relative mineral weathering rates. *Geochim. Cosmochim. Acta* **58**, 5019–5025.
- Brookins, D.G., 1989. Aqueous geochemistry of rare earth elements. In: Lippin, B.R., McKay, G.A. (Eds.), *Reviews in Mineralogy: Geochemistry and Mineralogy of Rare Earth Elements*, vol. 21. Mineral Society of America, Washington, DC, pp. 201–223.
- Byrne, R.H., Kim, K.H., 1990. Rare earth element scavenging in seawater. *Geochim. Cosmochim. Acta* **54**, 2645–2656.
- Byrne, R.H., Li, B.Q., 1995. Comparative complexation behavior of rare earths. *Geochim. Cosmochim. Acta* **59**, 4575–4589.
- Byrne, R.H., Sholkovitz, E.R., 1996. Marine chemistry and geochemistry of the lanthanides. In: Gschneidner, K.A., Jr., Eyring, L. (Eds.), *Handbook on the Physics and Chemistry of Rare Earth Elements*. Elsevier, Amsterdam, pp. 497–593.
- Byrne, R.H., Liu, X., 1998. A coupled riverine-marine fractionation model for dissolved rare earths and yttrium. *Aquat. Geochem.* **4**, 103–121.
- Chabaux, F., Riotte, J., Schmitt, A.-D., Carignan, J., Herckes, P., Pierret, M.-C., 2005. Variations of U and Sr isotope ratios in Alsace and Luxembourg rain waters: origin and hydrogeochemical implications. *CR Geosci.* **337** (16), 1447–1456.
- Dupré, B., Gaillardet, J., Rousseau, D., Allègre, C.J., 1996. Major and trace elements of river-borne material: The Congo basin. *Geochim. Cosmochim. Acta* **60** (8), 1301–1321.
- Elderfield, H., Upstill-Goddard, R., Sholkovitz, E.R., 1990. The rare earth elements in rivers, estuaries, and coastal seas and their significance to the composition of ocean waters. *Geochim. Cosmochim. Acta* **54**, 971–991.
- El Gh'Mari, A., 1995. Etude minéralogique, pétrophysique et géochimique de la dynamique d'altération d'un granite soumis au dépôts atmosphériques acides (Bassin versant du Strengbach, Vosges, France) mécanismes, bilans et modélisations. PhD Thesis, ULP Strasbourg, 202 p.
- Fichter, J., Turpault, M.P., Dambrine, E., Ranger, J., 1998. Mineral evolution of acid forest soils in the Strengbach catchment (Vosges mountains, N-E France). *Geoderma* **82**, 315–340.
- Gaillardet, J., Dupré, B., Allègre, C.J., 1995. A global geochemical mass budget applied to the Congo basin rivers: erosion rates and continental crust composition. *Geochim. Cosmochim. Acta* **59**, 3469–3485.
- Gaillardet, J., Dupré, B., Allègre, C.J., Nègre, P., 1997. Chemical and physical denudation in the Amazon river basin. *Chem. Geol.* **142**, 141–173.
- Goldstein, S.L., O'Nions, R.K., Hamilton, P.J., 1984. A Sm–Nd isotopic study of atmospheric dusts and particulates from major river systems. *Earth Planet. Sci. Lett.* **70**, 221–236.
- Goldstein, S.J., Jacobsen, S.B., 1987. The Nd and Sr isotopic systematics of river-water dissolved material: Implications for the sources of Nd and Sr in seawater. *Chem. Geol.* **66**, 245–272.
- Goldstein, S.J., Jacobsen, S.B., 1988a. Rare earth elements in river waters. *Earth Planet. Sci. Lett.* **89**, 35–47.
- Goldstein, S.J., Jacobsen, S.B., 1988b. Nd and Sr isotopic systematics of river water suspended material: implications for crustal evolution. *Earth Planet. Sci. Lett.* **87**, 249–265.
- Idir, S., Probst, A., Viville, D., Probst, J.L., 1999. Contribution des surfaces saturées et des versants aux flux d'eau et d'éléments exportés en période de crue: Traçage à l'aide du carbone organique dissous et de la silice. Cas du petit bassin versant du Strengbach (Vosges, France). *CR Acad. Sci.* **328**, 101–106.
- Ingri, J., Widerlund, A., Land, M., Gustafsson, Ö., Andersson, P., Öhlander, B., 2000. Temporal variations in the fractionation of the rare earth elements in a boreal river; the role of colloidal particles. *Chem. Geol.* **166**, 23–45.
- Johannesson, K.H., Tang, J., Daniels, J.M., Bounds, W.J., Burdige, D.J., 2004. Rare earth element concentrations and speciation in organic-rich blackwaters of the Great Dismal Swamp, Virginia, USA. *Chem. Geol.* **209**, 271–294.
- Krachler, M., Mohl, C., Emons, H., Shoty, W., 2003. Two thousand years of atmospheric rare earth element (REE) deposition as revealed by an ombrotrophic peat bog profile, Jura Mountains, Switzerland. *J. Environ. Monit.* **5**, 111–121.

- Ladouche, B., Probst, A., Viville, D., Idir, S., Baqué, D., Loubet, M., Probst, J.-L., Bariac, T., 2001. Hydrograph separation using isotopic, chemical and hydrological approaches (Strengbach catchment, France). *J. Hydrol.* **242**, 255–274.
- Li, Fuliang, Shan, Xiaoquan, Zhang, Tianhong, Zhang, Shuzhen, 1998. Evaluation of plant availability of rare earth elements in soils by chemical fractionation and multiple regression analysis. *Environ. Poll.* **102**, 269–277.
- Lu, P., Biron, P., Breda, N., Granier, A., 1995. Water relations of adult Norway spruce (*Picea abies* (L) Karst) under soil drought in the Vosges mountains: water potential, stomatal conductance and transpiration. *Ann. Sci. For.* **52**, 117–129.
- Martin, J.M., Meybeck, M., 1979. Element mass-balance of material carried by major world rivers. *Mar. Chem.* **7**, 173–206.
- Meybeck, M., 1987. Global chemical weathering from surficial rocks estimated from river dissolved loads. *Am. J. Sci.* **287**, 401–428.
- Négre, P., Allègre, C.J., Dupré, B., Lewin, E., 1993. Erosion sources determined by inversion of major and trace element ratios in river water: The Congo basin case. *Earth Planet. Sci. Lett.* **120**, 59–76.
- Öhlander, B., Ingri, J., Land, M., Schöberg, H., 2000. Change of Sm–Nd isotope composition during weathering of till. *Geochim. Cosmochim. Acta* **64**, 813–820.
- Ozaki, T., Enomoto, S., 2001. Uptake of rare earth elements by *Dryopteris erythrosora* (autumn fern). *Focused New Trends Bio-Trace Elem. Res.* **35**, 84–87.
- Prevosto, B., 1988. Flux des éléments minéraux dans un écosystème forestier déperissant. Impact de la pollution atmosphérique acide; Mémoire de 3^{ème} année. INRA, Champenoux-54280 Seichamps.
- Probst, A., Dambrine, E., Viville, D., Fritz, B., 1990. Influence of acid atmospheric inputs on surface water chemistry and mineral fluxes in a declining spruce stand within a small granitic catchment (Vosges massif, France). *J. Hydrol.* **116**, 101–124.
- Probst, A., Fritz, B., Viville, D., 1995. Mid-term trends in acid precipitation, streamwater chemistry and element budgets in the Strengbach catchment (Vosges mountains, France). *Water Air Soil Pollut.* **79**, 39–59.
- Probst, A., Viville, D., 1999. Bilan hydrogéochimique du petit bassin versant forestier du Strengbach à Aubure (Haut Rhin). In: *Rapport scientifique activités de recherche, 7^e réunion du conseil de direction scientifique*, Ifare/DFIU, 66–72.
- Riotte, J., Chabaux, F., 1999. (²⁴³U/²³⁸U) activity ratios in freshwaters as tracers of hydrological processes: the Strengbach watershed, Vosges, France. *Geochim. Cosmochim. Acta* **63**, 1263–1275.
- Rosbach, M., Jayasekera, R., Kniewald, G., Nguyen, Huu Thang, 1999. Large scale air monitoring: lichen vs. air particulate matter analysis. *Sci. Tot. Env.* **232**, 59–66.
- Scarascia-Mugnozza, G., Bauer, G.A., Persson, H., Mattaeucci, G., Masci, A., 2000. Tree biomass, growth and nutrient pools. In: Schulze, E.-D. (Ed.), *Carbon and Nitrogen Cycling in European Forest Ecosystems*. Springer, New York, pp. 49–62.
- Schmitt, A.-D., 2003. Les isotopes du calcium: développements analytiques-applications au bilan océanique présent et passé. Ph. D. Thesis, University of Strasbourg.
- Schmitt, A.-D., Chabaux, F., Stille, P., 2003. The calcium riverine and hydrothermal isotopic fluxes and the oceanic calcium mass balance. *Earth Planet. Sci. Lett.* **213**, 503–518.
- Schmitt, A.-D., Stille, P., 2005. The source of calcium in wet atmospheric deposits: Ca–Sr isotope evidence. *Geochim. Cosmochim. Acta* **69**, 3463–3468.
- Shabani, M.B., Masuda, A., 1991. Sample introduction by on-line two-stage solvent extraction and back-extraction to eliminate matrix interference and to enhance sensitivity in the determination of rare earth elements with inductively coupled plasma spectrometry. *Anal. Chem.* **63**, 2099–2105.
- Sholkovitz, E.R., 1992. Chemical evolution of rare earth elements: fractionation between colloidal and solution phases of filtered river water. *Earth Planet. Sci. Lett.* **114**, 77–84.
- Sholkovitz, E.R., 1993. The geochemistry of rare earth elements in the Amazon river estuary. *Geochim. Cosmochim. Acta* **57**, 2181–2190.
- Sholkovitz, E.R., Landing, W.M., Lewis, B.L., 1994. Ocean particle chemistry: the fractionation of rare earth elements between suspended particles and seawater. *Geochim. Cosmochim. Acta* **58**, 1567–1579.
- Sholkovitz, E.R., 1995. The aquatic chemistry of rare earth elements in rivers and estuaries. *Aquat. Geochem.* **1**, 1–34.
- Soulsby, C., 1992. Hydrological controls on acid runoff generation in a forested headwater catchment at Llyn Brienne, Mid-Wales. *J. Hydrol.* **138**, 431–448.
- Soulsby, C., 1995. Contrasts in storm event hydrochemistry in an afforested catchment in Upland Wales. *J. Hydrol.* **170**, 159–179.
- Stallard, R.F., Edmond, J.M., 1983. Geochemistry of the Amazon 2. The influence of geology and weathering environment on the dissolved load. *J. Geophys. Res.* **88**, 9671–9688.
- Steinmann, M., Stille, P., 1997. Rare earth element behavior and Pb, Sr, Nd isotope systematics in a heavy metal contaminated soil. *Appl. Geochem.* **12**, 607–624.
- Stille, P., Clauer, N., 1994. The process of glauconitization: chemical and isotopic evidence. *Contrib. Mineral. Petrol.* **117**, 253–262.
- Stille, P., Gauthier-Lafaye, F., Jensen, K.A., Salah, S., Bracke, G., Ewing, R.C., Louvat, D., Million, D., 2003. REE mobility in groundwater proximate to the natural fission reactor at Bangombé (Gabon). *Chem. Geol.* **198**, 289–304.
- Stordal, M.C., Wasserburg, G.J., 1986. Neodymium isotopic study of Baffin Bay water: sources of REE from very old terranes. *Earth Planet. Sci. Lett.* **77**, 259–272.
- Sun, H., Wang, X., Wang, Q., Wang, H., Chen, Y., Dai, L.C., 1999. The effects of chemical species on bioaccumulation of rare earth elements in rice grown in nutrient solution. *Toxicol. Environ. Chem.* **69**, 75–85.
- Tricca, A., 1997. Transport mechanism of trace elements in surface and groundwater: Sr, Nd, U isotope and REE evidence. PhD Thesis, University of Strasbourg.
- Tricca, A., Stille, P., Steinmann, M., Kiefel, B., Samuel, J., Eikenberg, J., 1999. Rare earth elements and Sr and Nd isotopic compositions of dissolved and suspended loads from small river systems in the Vosges mountains (France), the river Rhine and the groundwater. *Chem. Geol.* **160**, 139–158.
- Viers, J., Dupré, B., Polvé, M., Schott, J., Dandurand, J.-L., Braun, J.-J., 1997. Chemical weathering in the drainage basin of a tropical watershed (Nsimi-Zoété site, Cameroon): comparison between organic-poor and organic-rich waters. *Chem. Geol.* **140**, 181–206.
- Viville, D., Biron, P., Granier, A., Dambrine, E., Probst, A., 1993. Interception in a mountainous declining spruce stand in the Strengbach catchment (Vosges, France). *J. Hydrol.* **144**, 273–282.
- Wallander, H.K., Wickman, T., Jacks, G., 1997. Apatite as a P source in mycorrhizal and non-mycorrhizal *Pinus sylvestris* seedlings. *Plant Soil* **196** (1), 123–131.
- Yang, L., Wang, X., Sun, H., Zhang, H., 1999. The effect of EDTA on rare earth elements bioavailability in soil ecosystem. *Chemosphere* **38**, 2825–2833.
- Zeng, F., Tian, H.E., Wang, Z., An, Y., Gao, F., Zhang, L., Li, F., Shan, L., 2003. Effect of rare earth element europium on amaranthin synthesis in *Amaranthus caudatus* seedlings. *Biol. Trace Elem. Res.* **93**, 271–282.
- Zhang, Z.Y., Wang, Y.Q., Li, F.L., Xiao, H.Q., Chai, Z.F., 2002. Distribution characteristics of rare earth elements in plants from a rare earth ore area. *J. Radioanal. Nucl. Chem.* **252**, 461–465.
- Zhimang, G., Xiaorong, W., Jing, C., Liansheng, W., Lemei, D., 2000. Effects of sulfate on speciation and bioavailability of rare earth elements in nutrient solution. *Chem. Spec. Bioavailab.* **12**, 53–58.